

# Quantum probes for ohmic environments at thermal equilibrium

Fahimeh Salari Sehbaran<sup>1</sup> and Matteo Bina, Claudia Benedetti, Matteo G. A. Paris<sup>2</sup>

<sup>1</sup>*Faculty of Physics, Shahid Bahonar University of Kerman, Kerman, Iran*

<sup>2</sup>*Quantum Technology Lab, Dipartimento di Fisica Aldo Pontremoli, Università di Milano, I-20133 Milano, Italy*

It is often the case that the environment of a quantum system may be described as a bath of oscillators with Ohmic density of states. In turn, the precise characterization of these classes of environments is a crucial tool to engineer decoherence or to tailor quantum information protocols. Recently, the use of quantum probes in characterizing Ohmic environments at zero-temperature has been discussed, showing that a single qubit provides precise estimation of the cutoff frequency. On the other hand, thermal noise often spoil quantum probing schemes, and for this reason we here extend the analysis to complex system at thermal equilibrium. In particular, we discuss the interplay between thermal fluctuations and time evolution in determining the precision attainable by quantum probes. Our results show that the presence of thermal fluctuations degrades the precision for low values of the cutoff frequency, i.e. values of the order  $\omega_c \lesssim T$  (in natural units). For larger values of  $\omega_c$  decoherence is mostly due to the structure of environment, rather than thermal fluctuations, such that quantum probing by a single qubit is still an effective estimation procedure.

## I. INTRODUCTION

In the last decade, technological advances in control and manipulation of quantum systems have made quantum probes available to the characterization of a large set of physical platforms. In turn, a radically new approach emerged to probe complex quantum systems, which is based on the quantification and optimisation of the information that can be extracted by an immersed quantum probe as opposed to a classical one [1–9]. Quantum probes offer two main advantages: on one hand, they often provide enhanced precision, due to the inherent sensitivity of quantum system to environment-induced decoherence. On the other hand, they provide non invasive techniques in order to estimate parameters of interest, without perturbing too much the system under investigation.

In this paper, we address the use of the simplest quantum probe, a single qubit, as it already embodies all the desired properties of an effective probe: it is small, only weakly invasive, and it can be easily manipulated and controlled [10–12]. Our aim is to characterize the spectral properties of a bath of oscillators, which itself provides a quite general model, suitable to describe several complex systems of interest for quantum information science and reservoir engineering [13–18]. In particular, we focus on the cut-off frequency  $\omega_c$  of the environment, which is linked to the environment correlation time and, in turn, to

the available coherence time for communication and computation. Indeed, a precise characterization of the spectral density is a crucial step to the engineering of reservoirs, tailored to specific tasks. Recently, the effective use of a single qubit quantum probe to characterize Ohmic environments at zero-temperature has been analyzed and discussed [3]. On the other hand, thermal fluctuations often spoil the effectiveness of quantum metrological protocols, the most dramatic case being represented by quantum interferometry, where an infinitesimal amount of noise is enough to kill Heisenberg scaling and reinstates the shot noise limit [19]. In turn, the effect of temperature has been analyzed in different metrological contexts, for example the out-of-equilibrium regimes [20] and phase estimation in Gaussian states [21]. For these reasons, we extend here the analysis to the more realistic case of complex systems at thermal equilibrium, and discuss in details the interplay among thermal fluctuations and time evolution in making the qubit an effective probe for the cutoff frequency of its environment. In this context, a relevant feature of our probing technique is the pure dephasing nature of the interaction between the qubit and its environment. This means that while the Ohmic system has a fixed temperature, the probe has access to the full set of out-of-equilibrium states [22], while not exchanging energy with the Ohmic system. As we will see, this provides room to optimise the probing strategy and to enhance sensitivity over classical (thermal) probes.

Any probing strategy requires control of the initial state of the probing system, as well as of the coupling with the probed one. Concerning the detection of the probe after interaction, we exploit results from local quantum estimation theory (QET), which provides the necessary tools to determine the most informative measurement and the most precise estimator and, in turn, to optimise the extraction of information from the quantum probe [23]. Indeed, QET has been effectively employed in different contexts [24–44], in order to individuate the most convenient detection scheme, and to evaluate the ultimate quantum bounds to precision. In this work, we address the characterization of Ohmic environments at thermal equilibrium, i.e. the estimation of their cutoff frequency, assuming that the nature of the environment is known, i.e. the value of the ohmicity parameter. On the other hand, we optimize the strategy over the initial preparation of the probe qubit, the interaction time and the detection scheme at the output. In particular, we pay attention to the overall estimability of the cutoff frequency, as measured by the quantum signal-to-noise ratio, in different temperature regimes. As we will see, the presence of thermal fluctuations degrades the estimation precision. On the other hand, the negative effects of temperature are relevant only for small values of the cutoff frequency, i.e. values of the order  $\omega_c \lesssim T$  (in natural units). For larger values of the cutoff frequency the decoherence of the probe is mostly due to the structure of the environment, rather than thermal fluctuations, and therefore the overall estimation procedure is still very effective, with performances very close to the zero temperature case.

The paper is structured as follows. In Section II, we describe the interaction model, establish notation,

and briefly review the ideas and the tools of QET. In Sec. III we present our results and discuss in details the interplay between thermal fluctuations and time evolution in determining the precision of quantum probes. Section IV closes the paper with some concluding remarks.

## II. THE MODEL

Our quantum probe is a single qubit with energy gap  $\omega_0$ , which interacts with a bosonic reservoir at thermal equilibrium. The total Hamiltonian may be written as

$$\mathcal{H} = \frac{\omega_0}{2} \sigma_3 + \sum_k \omega_k b_k^\dagger b_k + \sigma_3 \sum_k (g_k b_k^\dagger + g_k^* b_k), \quad (1)$$

where  $\omega_k$  is the frequency of the  $k$ -th reservoir mode and we use natural units with  $\hbar = k_B = 1$ . The Pauli matrix  $\sigma_3$  acts on the qubit and  $[b_k, b_k^\dagger] = \delta_{k,k'}$  describes the modes of the bath. The  $g_k$ 's are coupling constants, describing the interaction of each mode with the qubit. Their distribution is usually described in terms of the so-called spectral density of the bath, which is defined as  $J(\omega) = \sum_k |g_k|^2 \delta(\omega_k - \omega)$ . The spectral density depends on the specific features of the physical system and may be often engineered in order to enable control of quantum decoherence [2]. The model described by  $\mathcal{H}$  in Eq. (1) is exactly solvable, making it possible to analyze the mechanisms creating entanglement between the qubit and environment, which in turn is at the core of decoherence processes [1, 2].

We are interested in probing properties of the environment by performing measurements on the qubit. To this aim, we study the reduced dynamics of the qubit assuming that the environment is at thermal equilibrium, i.e.

$$\rho_E = \frac{1}{Z} \exp \left\{ -\frac{1}{T} \sum_k \omega_k b_k^\dagger b_k \right\},$$

where  $Z = \text{Tr} \left[ \exp \left\{ -\frac{1}{T} \sum_k \omega_k b_k^\dagger b_k \right\} \right]$  is the partition function and  $T$  denotes the temperature. In particular, our goal is to probe the cutoff frequency of Ohmic environments, i.e. the quantity  $\omega_c$  appearing in spectral densities of the form

$$J_s(\omega, \omega_c) = \omega_c \left( \frac{\omega}{\omega_c} \right)^s \exp \left\{ -\frac{\omega}{\omega_c} \right\}. \quad (2)$$

The cutoff frequency is a crucial parameter for applications in quantum information science, since it is linked to the environment correlation time and, in turn, to the available coherence time for communication and computation. The quantity  $s$  is a real positive number, which instead governs the behaviour of the spectral density at low frequencies. Upon varying  $s$  we move from the sub-Ohmic regime ( $s < 1$ ), to Ohmic

( $s = 1$ ), and to super-Ohmic one ( $s > 1$ ). In the following, in order to make some explicit quantitative statements, we will often refer to the paradigmatic values  $s = 0.5, 1, 3$  [45, 46].

The initial state of the combined system, qubit and environment, is described by the density matrix

$$\rho_{QE}(0) = \rho_Q(0) \otimes \rho_E \quad (3)$$

where  $\rho_E$  is given above. The initial preparation of the qubit probe  $\rho_Q(0)$  should be optimised in order to extract the maximum possible information on  $\omega_c$  from measurements performed on the qubit after the interaction with the environment. This optimization has been performed in Ref. [3] for environments at zero temperature. The proof does not depend on the structure of the environment, but only on the pure dephasing map of the qubit. Since the same dynamical map is considered here, the proof holds also for thermal environments, and thus we consider  $\rho_Q(0) = |+\rangle\langle+| = \frac{1}{2}(\mathbb{I} + \sigma_1)$ , where  $|+\rangle = \frac{1}{\sqrt{2}}(|0\rangle + |1\rangle)$ , being  $\{|0\rangle, |1\rangle\}$  the computational basis, i.e. the eigenstates of  $\sigma_3$ . We now move to the interaction picture, where the Hamiltonian and the evolution operator take on the expressions:

$$\mathcal{H}_I = \sigma_3 \sum_k \left( g_k b_k^\dagger e^{i\omega_k \tau} + g_k^* b_k e^{-i\omega_k \tau} \right) \quad (4)$$

$$U_I(\tau) \propto \exp \left[ \frac{1}{2} \sigma_3 \sum_k \left( \alpha_k b_k^\dagger - \alpha_k^* b_k \right) \right] \quad (5)$$

where  $\alpha_k = 2g_k \frac{1 - e^{i\omega_k \tau}}{\omega_k}$  [1]. If we assume a continuum of environment's modes, we can use the spectral density (2) to evaluate the evolved state of the qubit probe upon tracing out the environment  $\rho_Q(\tau) = \text{Tr}_E \left[ U_I(\tau) \rho_{QE}(0) U_I^\dagger(\tau) \right]$ , which explicitly reads:

$$\rho_Q(\tau) = \frac{1}{2} \left( \mathbb{I} + e^{-\Gamma_s(\tau, T, \omega_c)} \sigma_1 \right), \quad (6)$$

where

$$\Gamma_s(\tau, T, \omega_c) = \int_0^\infty d\omega J_s(\omega, \omega_c) \frac{1 - \cos \omega \tau}{\omega^2} \coth \left( \frac{\omega}{2T} \right), \quad (7)$$

is usually referred to as the *decoherence function*, with  $\exp\{-\Gamma_s(\tau, T, \omega_c)\}$  referred to as the decoherence factor. Notice that in Eq. (7) frequencies, time and temperature are dimensionless quantities expressed in units of the probe frequency  $\omega_0$ . The decoherence function depends on the temperature  $T$  of the environment, and on the form of the spectral density  $J_s(\omega, \omega_c)$  [1, 3], i.e. on the cutoff frequency  $\omega_c$  and the ohmicity parameter  $s$ . An analytic form of the integral in Eq. (7) may be obtained at any temperature, time and Ohmicity parameter by expanding the hyperbolic cotangent  $\coth(x) = 1 + 2 \sum_{n=1}^\infty e^{-2nx}$ . Then, the decoherence function may be written as

$$\Gamma_s(\tau, T, \omega_c) = \Gamma_s(\tau, 0, \omega_c) + 2 \sum_{n=1}^\infty \left( \frac{T}{T + n\omega_c} \right)^{s-1} \Gamma_s \left( \tau, 0, \frac{T\omega_c}{T + n\omega_c} \right),$$

which explicitly reads

$$\Gamma_s(\tau, T, \omega_c) = \Gamma_s(\tau, 0, \omega_c) + s(s-1) \left( \frac{T}{\omega_c} \right)^{s-1} \frac{\Gamma_e[s-1]^2}{\Gamma_e[s+1]} F(\zeta) \quad (8)$$

where  $\Gamma_e[z] = \int_0^\infty dt t^{z-1} e^{-t}$  is the Euler Gamma function and where we introduced the function

$$F(\zeta) \equiv 2\zeta[s-1, 1+\text{Re}(w)] - \zeta[s-1, 1+w] - \zeta[s-1, 1+w^*], \quad (9)$$

where  $w \equiv T\omega_c^{-1} + iT\tau$ ,  $\zeta[p, q] = \sum_{k=0}^\infty (k+q)^{-p}$  is the generalised (Hurwitz) Zeta function and  $\Gamma_s(\tau, 0, \omega_c)$  is the decoherence function at zero temperature, i.e. [3]

$$\Gamma_s(\tau, 0, \omega_c) = \Gamma_e[s-1] \left\{ 1 - \frac{\cos[(s-1) \arctan(\omega_c \tau)]}{(1 + \omega_c^2 \tau^2)^{\frac{s-1}{2}}} \right\}. \quad (10)$$

The behaviour of the decoherence function, that from now on we denote as  $\Gamma_s \equiv \Gamma_s(\tau, T, \omega_c)$ , as a function of the dimensionless time  $\tau$  is shown in Fig. 1, for different cutoff frequencies, Ohmicity parameters and two regimes of high and low temperature of the environment. As it is apparent from the plots, for short times ( $\tau \ll 1$ ) the decoherence function follows a power-law scaling for any value of the other parameters. More precisely, from a first-order approximation, it scales as  $\tau^2$ :

$$\Gamma_s \simeq \frac{1}{2} \omega_c^2 \Gamma_e(s-1) \left[ 2 \left( \frac{T}{\omega_c} \right)^{s+1} \zeta\left(s+1, \frac{T}{\omega_c}\right) - 1 \right] \tau^2. \quad (11)$$

The asymptotic behaviour at long times, instead, is different for the three choices of the Ohmicity parameters. In particular, in the super-Ohmic case with  $s = 3$  the decoherence function saturates to a constant value, at any temperature  $T$ . This means that the stationary state of the qubit is not a fully dephased one, and that the residual degree of coherence is larger for values of the parameters leading to smaller saturation values of  $\Gamma_3$ . In the other cases, sub-Ohmic with  $s = 0.5$  and Ohmic with  $s = 1$ , the decoherence function scales, respectively, as  $\Gamma_{0.5} \sim \tau^{\frac{3}{2}}$  and  $\Gamma_1 \sim \tau$ , meaning that the stationary state of the qubit probe has been completely decohered. The long-time behavior of the decoherence function is also important from the point of view of the characterization of the type of Ohmic-like environment, namely the asymptotic scaling clearly distinguishes and characterizes the Ohmicity parameter of the considered structured reservoir.

### A. Quantum parameter estimation

The density matrix  $\rho_Q(\tau, \omega_c, s, T)$  in Eq. (6) describes the state of the qubit probe after the interaction with the environment. As such, it depends on the interaction time  $\tau$ , which is basically a free parameter, on the temperature  $T$  and the Ohmicity parameter  $s$ , which are fixed by the experimental conditions, and on the cutoff frequency  $\omega_c$  of the environment, which is the parameter we would like to estimate. In the jargon of

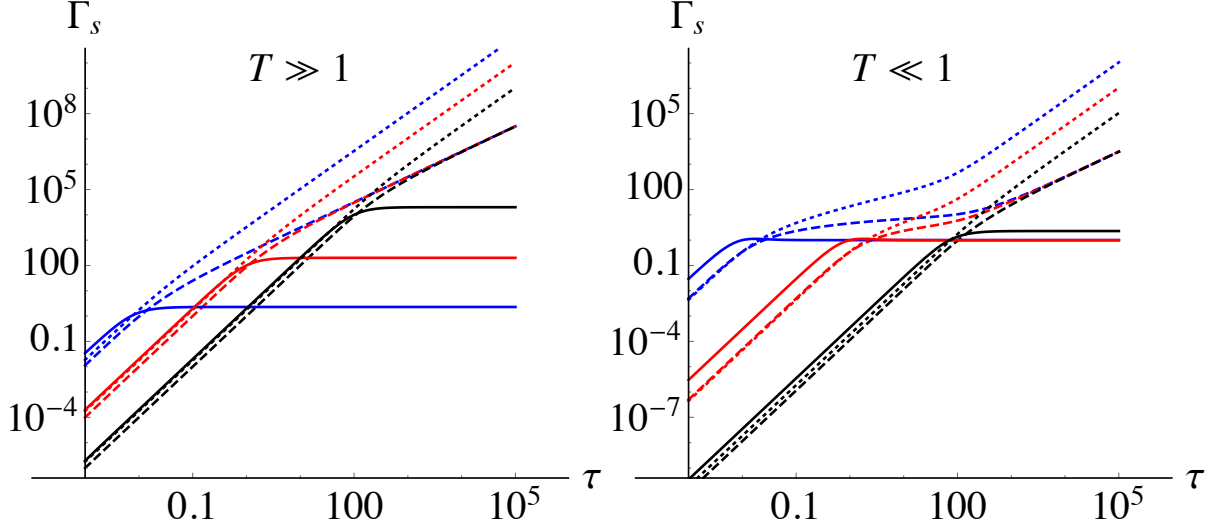


FIG. 1: Decoherence function  $\Gamma_s$  as a function of the dimensionless time  $\tau$  for different temperatures, cutoff frequencies, and ohmicity parameters. The left panel reports  $\Gamma_s$  in the high temperature regime (the plot is for  $T = 10^2$ ), whereas the right panel shows it for low temperature,  $T = 10^{-2}$ . In both plots, black lines are for  $\omega_c = 10^{-2}$ , red ones for  $\omega_c = 1$  and blue ones for  $\omega_c = 10^2$ . Finally, solid lines denote results obtained for super-Ohmic environments ( $s = 3$ ), dashed for Ohmic ( $s = 1$ ) and dotted ones for sub-Ohmic ( $s = 0.5$ ).

quantum estimation, it is usually referred to as a *quantum statistical model*. According to this classification, and in order to simplify the notation, in this Section we will use the following shorthands

$$\rho_Q(\tau, \omega_c, s, T) \longrightarrow \rho_c \quad \frac{\partial}{\partial \omega_c} \longrightarrow \partial_c.$$

Our task is to optimize the inference of  $\omega_c$  by performing measurements on  $\rho_c$ . To this aim, we employ results from quantum estimation theory [23], which provides tools to find the best detection scheme and to evaluate the corresponding lower bounds to precision. We assume that the value of the temperature  $T$  and the Ohmicity parameter  $s$  are fixed, whereas the value of interaction time is a free parameter, over which we may further optimize the precision.

Let us consider the family of quantum states  $\rho_c$ , which is labeled by the cutoff frequency  $\omega_c$ . In order to estimate  $\omega_c$  we perform measurements on repeated preparations of the quantum probe and then process the overall sample of outcomes. Let us denote by  $X$  the observable measured on the probe, and by  $p(x|c)$  the conditional distribution of its outcomes when the true value of the cutoff frequency is  $\omega_c$ . We also denote by  $M$  the number of repeated measurements. Once  $X$  is chosen and a set of outcomes  $\mathbf{x} = \{x_1, \dots, x_M\}$  is collected, we process the data by an *estimator*  $\hat{\omega}_c \equiv \hat{\omega}_c(\mathbf{x})$ , i.e. a function from the space of datasets to the manifold of the parameter values. The *estimate* of the cutoff frequency is the average value of the estimator

over data, whereas the *precision* of this estimate corresponds to the variance of the estimator i.e.

$$\bar{\omega}_c = \int d\mathbf{x} p(\mathbf{x}|c) \hat{\omega}_c(\mathbf{x}), \quad V_c \equiv \text{Var } \omega_c = \int d\mathbf{x} p(\mathbf{x}|c) [\hat{\omega}_c(\mathbf{x}) - \bar{\omega}_c]^2, \quad (12)$$

where  $p(\mathbf{x}|c) = \prod_{k=1}^M p(x_k|c)$ , since the repeated measurements are independent on each other. The smaller is  $V_c$ , the more precise is the estimator. In fact, there is a bound to the precision of any unbiased estimator (those satisfying the condition  $\bar{\omega}_c \rightarrow \omega_c$  for  $M \gg 1$ ), given by the Cramér-Rao (CR) inequality:

$$V_c \geq \frac{1}{MF_c}, \quad F_c = \int dx p(x|c) [\partial_c \log p(x|c)]^2, \quad (13)$$

where  $F_c$  is the (single-measurement) Fisher information (FI). The best, i.e. more precise, measurement to infer the value of  $\omega_c$  is the measurement maximising the FI, where the maximization should be performed over all the possible observables of the probe. To this aim, one introduces the symmetric logarithmic derivative  $L_{\omega_c} \equiv L_c$  (SLD), as the operator which satisfies the relation

$$L_c \rho_c + \rho_c L_c = 2\partial_c \rho_c. \quad (14)$$

The quantum CR theorem states that the optimal quantum measurements are those corresponding to the spectral measure of the SLD, and consequently  $F_c \leq H_c = \text{Tr}[\rho_c L_c^2]$ , where  $H_c$  is usually referred to as the quantum Fisher information (QFI). The quantum CR inequality then follows

$$V_c \geq \frac{1}{MH_c} \quad (15)$$

and it represents the ultimate bound to precision, taking into account both the intrinsic (quantum), and extrinsic (statistical), source of fluctuations for the estimator. Starting from the diagonal form of the quantum statistical model  $\rho_c = \sum_n \rho_n |\phi_n\rangle\langle\phi_n|$ , where both the eigenvalues and the eigenvectors do, in general, depend on the parameter of interest, we arrive at a convenient form of the QFI

$$H_c = \sum_n \frac{(\partial_c \rho_n)^2}{\rho_n} + 2 \sum_{n \neq m} \frac{(\rho_n - \rho_m)^2}{\rho_n + \rho_m} |\langle\phi_m|\partial_c \phi_n\rangle|^2 \quad (16)$$

where, for our qubit case,  $n, m = 1, 2$ . The first term in Eq. (16) is the FI of the distribution of the eigenvalues  $\rho_n$ , whereas the second term is a positive definite, genuinely quantum, contribution, explicitly quantifying the potential quantum enhancement of precision. Any measurement  $X$  on the system is associated to its FI, and different measurements lead to different degrees of precisions through the CR bound. However, when a measurement is found, such that the condition  $F_c = H_c$  is satisfied, the measurement is said to be *optimal*. If the equality in Eq. (15) is satisfied the corresponding estimator is said to be *efficient*. A global measure of the estimability of a parameter, weighting the variance with the value of the parameter,

is given by the signal-to-noise ratio  $R_c = \omega_c^2/V_c$ . The quantum CR bound may then be rewritten in terms of  $R_c$  as follows

$$R_c \leq Q_c = \omega_c^2 H_c, \quad (17)$$

where  $Q_c$  is referred to as the quantum signal-to-noise ratio (QSNR), and itself represents the ultimate quantum bound to the estimability of a parameter [9, 23]. The larger is the QSNR, the (potentially) more effective is the estimation scheme [3]. Here "potentially" refers to the fact that a large value of the QSNR means a large QFI, which in turn tells us about the maximum precision that can be achieved. However, it does not say anything about the best estimator that must be employed in order to process the output data and to infer the value of the parameter. A large  $Q_c$  is a necessary step in order to precisely estimate the parameter. Finally, we notice that  $\omega_c$  takes value on a subset of the real axis and this means that even if the optimal measurement does depend on the value to be estimated, the ultimate precision dictated by the quantum Cramer-Rao bound may be achieved by a two-stage adaptive scheme [47].

### III. QUANTUM PROBES FOR OHMIC ENVIRONMENTS AT THERMAL EQUILIBRIUM

In this section, using results of Section II, we discuss the performances of a qubit probe in estimating the cutoff frequency of Ohmic environments at thermal equilibrium. Our starting point is the state of the probe after the interaction with the environment, which provides the quantum statistical model  $\rho_c$ . We assume that the temperature  $T$  and the Ohmicity parameter  $s$  are fixed by the experimental conditions, whereas the interaction time  $\tau$  may be tuned in order to maximise the quantum Fisher information  $H_c$  and, in turn, the quantum signal-to-noise ratio  $Q_c$ . To this aim, we first diagonalize  $\rho_c$  and then use Eq. (16). After some algebra, we arrive at

$$H_c(\tau) = \frac{[\partial_c \Gamma_s]^2}{\exp[2\Gamma_s] - 1}, \quad (18)$$

where we have omitted the explicit dependence on  $T$  and  $\Gamma_s$  is given by the explicit analytic formula (8). Starting from Eq. (18) we have maximised  $Q_c(\tau) = \omega_c^2 H_c(\tau)$  over the interaction time  $\tau$  at different fixed values of  $T$  and  $s$ . In particular, we have considered three specific values of  $s = 0.5, 1, 3$  in order to address sub-Ohmic, Ohmic, and super-Ohmic regimes.

In Fig. 2 we show the results of the optimisation. The upper plots show the optimal interaction time  $\tau_c$  as a function of the cutoff frequency for the three considered values of the Ohmicity parameter, and for different values of temperature ( $T = 0.1, 0.5, 1.0, 5.0, 10.0$ ), whereas the plots in the lower panels show the corresponding optimised values of the QSNR  $Q_c$ , for the same values of  $s$  and  $T$ . In all the plots, the



arrow denotes increasing values of temperature. In the region of low cutoff frequencies, the decoherence of the probe qubit is governed by thermal fluctuation, rather than the structure of the environment. As a consequence, a larger interaction time, scaling as  $\tau_c \propto \omega_c^{-1/2}$ , is needed to imprint the maximal possible information about  $\omega_c$  on the probe. The corresponding values of  $Q_c$  are anyway smaller than those achievable in the zero temperature case, which corresponds to the upper saturation level for  $\omega_c \gg T$ . Upon increasing the cutoff frequency, the zero temperature scaling of the optimal time,  $\tau_c \propto \omega_c^{-1}$  is recovered, as well as the values of the optimised QSNR. Combining numerical results with Eq. (8) we see that for  $\omega_c > T$  the optimal time scales as follows:  $\tau_c \simeq \frac{5}{4} \omega_c^{-1}$  for  $s = 0.5$ ,  $\tau_c \simeq \omega_c^{-1}$  for  $s = 1$ , and  $\tau_c \simeq \frac{2}{5} \omega_c^{-1}$  for  $s = 3$ , independently on the temperature itself.

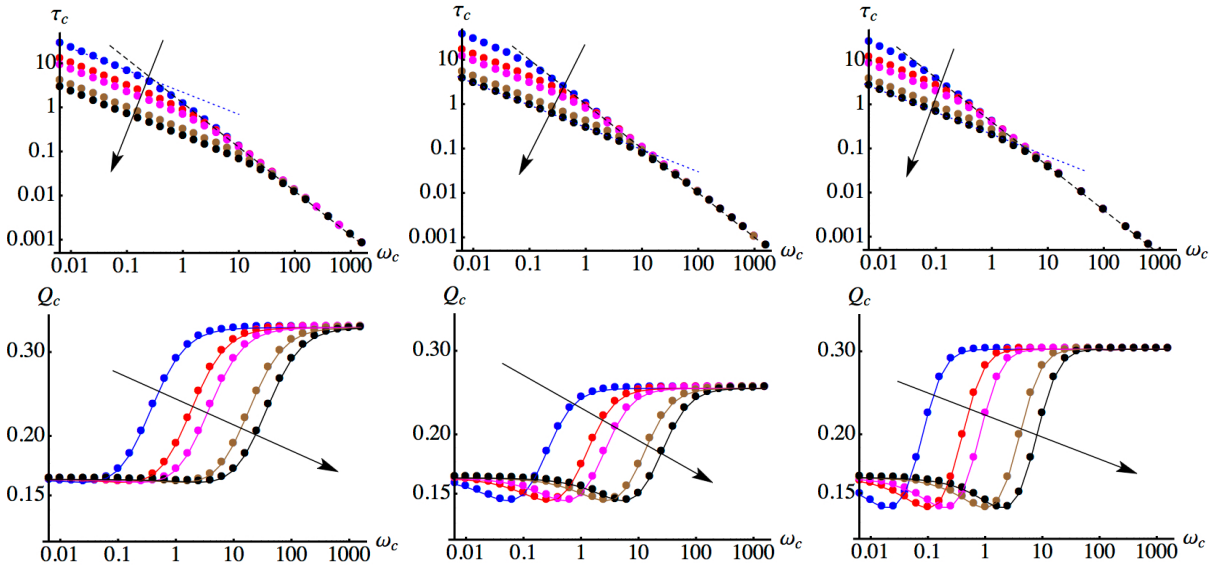


FIG. 2: Upper plots: the optimal interaction time  $\tau_c$  as a function of the cutoff frequency  $\omega_c$  for different values of the temperature (from top to bottom we have  $T = 0.1, 0.5, 1.0, 5.0, 10.0$ , arrows point to increasing temperature). From left to right the plots refer to  $s = 0.5, 1, 3$ . Dashed lines indicate the scaling of  $\tau_c$  with  $\omega_c$  in the two regimes of low and high cutoff frequency. Lower plots: the optimised values of the QSNR  $Q_c$ , achieved for the interaction times of the upper plots, as a function of the cutoff frequency for different values of the temperature (from top to bottom we have  $T = 0.1, 0.5, 1.0, 5.0, 10.0$ , arrows point to increasing temperature). From left to right the plots refer to  $s = 0.5, 1, 3$ .

The transition from the regime of decoherence induced by temperature to the regime of decoherence governed by the structure of the environment may be traced back to the behaviour of the decoherence function  $\Gamma_s$ , and takes place for cutoff frequencies of the order  $\omega_c \simeq T$ . Remarkably, as far as  $\omega_c$  is exceeding this threshold value, the value of the QSNR  $Q_c$  quickly increases, and reach the zero temperature level independently on the temperature of the environment. We notice that even in the region of low cutoff

frequencies where thermal fluctuations degrade performances (the QSNR is reduced by a factor about 2/3), qubit probes are still providing information about their environment.

#### IV. CONCLUSIONS

In this paper, we have addressed estimation of the cutoff frequency of a complex Ohmic environment at thermal equilibrium. Our approach is based on the use of a quantum probe, i.e. a simple quantum system which undergoes decoherence due to its interaction with the environment. In particular, we have focussed on the use of a single qubit subject to environment-induced dephasing, and have evaluated the optimal interaction time between the probe and the environment, needed to imprint on the qubit the maximum information about the cutoff frequency. In addition, we have discussed the interplay between thermal fluctuations and time evolution in determining the precision of quantum probes.

Our results shows that the presence of thermal fluctuations degrades the precision for low values of the cutoff frequency, whereas for larger values a single qubit is still providing nearly optimal performances, i.e. precision close to the zero temperature case. This behaviour may be explained in terms of the mechanisms responsible for the decoherence of the qubit. In the region of low cutoff frequencies, the decoherence of the probe is governed by thermal fluctuations, rather than the structure of the environment. As a consequence, a larger interaction time, scaling as  $\tau_c \propto \omega_c^{-1/2}$ , is needed to imprint the maximal possible information about  $\omega_c$  on the probe, and the corresponding values of the QSNR are smaller than those achievable in the zero temperature case. On the other hand, upon increasing the cutoff frequency, thermal fluctuations are no longer the main cause of decoherence, and the zero temperature scaling of the optimal interaction time,  $\tau_c \propto \omega_c^{-1}$  is recovered, as well as the values of the optimised QSNR. Our results pave the way for possible applications to realistic room temperature systems, as well as for estimation of more than a single parameter in system-environment couplings with general spectra.

#### Acknowledgments

The authors thank Luigi Seveso and Sholeh Razavian for several useful discussions. This work has been supported by EU through the collaborative H2020 project QuProCS (Grant No. 641277) and by SERB

through project VJR/2017/000011. MGAP is member of GNFM-INdAM.

- 
- [1] Breuer, H.-P.; Petruccione, F. *The Theory of Open Quantum Systems*; Oxford University Press: New York, NY, USA, 2002.
  - [2] Palma, M.G.; Suominen, K.-A.; Ekert, A.K. Quantum computers and dissipation. *Proc. R. Soc. Lond. A* **1996**, *452*, 567–584.
  - [3] Benedetti, C.; Sehgaran, F.S.; Zandi, M.H.; Paris, M.G.A. Quantum probes for the cutoff frequency of Ohmic environments. *Phys. Rev. A* **2018**, *97*, 012126.
  - [4] Bina, M.; Grasselli, F.; Paris, M.G.A. Continuous-variable quantum probes for structured environments. *Phys. Rev. A* **2018**, *97*, 012125.
  - [5] Elliott, T.J.; Johnson, T.H. Nondestructive probing of means, variances, and correlations of ultracold-atomic-system densities via qubit impurities. *Phys. Rev. A* **2016**, *93*, 043612.
  - [6] Streif, M.; Buchleitner, A.; Jaksch, D.; Mur-Petit, J. Measuring correlations of cold-atom systems using multiple quantum probes. *Phys. Rev. A* **2016**, *94*, 053634.
  - [7] Troiani, F.; Paris, M.G.A. Probing molecular spin clusters by local measurements. *Phys. Rev. B* **2016**, *94*, 115422.
  - [8] Cosco, F.; Borrelli, M.; Plastina, F.; Maniscalco, S. Momentum-resolved and correlation spectroscopy using quantum probes. *Phys. Rev. A* **2017**, *95*, 053620.
  - [9] Benedetti, C.; Buscemi, F.; Bordone, P.; Paris, M.G.A. Quantum probes for the spectral properties of a classical environment. *Phys. Rev. A* **2014**, *89*, 032114.
  - [10] Zhang, J.; Peng, X.; Rajendran, N.; Suter, D. Detection of Quantum Critical Points by a Probe Qubit. *Phys. Rev. Lett.* **2008**, *100*, 100501.
  - [11] Berkley, A.J.; Przybysz, A. J.; Lanting, T.; Harris, R.; Dickson, N.; Altomare, F.; Amin, M. H.; Bunyk, P.; Enderud, C.; Hoskinson, E.; et al. Tunneling spectroscopy using a probe qubit. *Phys. Rev. B* **2013**, *87*, 020502(R).
  - [12] Lolli, J.; Baksic, A.; Nagy, D.; Manucharyan, V.E.; Ciuti, C. Ancillary Qubit Spectroscopy of Vacua in Cavity and Circuit Quantum Electrodynamics. *Phys. Rev. Lett.* **2015**, *114*, 183601.
  - [13] Paavola, J.; Piilo, J.; Suominen, K.-A.; Maniscalco, S. Environment-dependent dissipation in quantum Brownian motion. *Phys. Rev. A* **2009**, *79*, 052120.
  - [14] Martinazzo, R.; Hughes, K.H.; Martelli, F.; Burghard, I. Effective spectral densities for system-environment dynamics at conical inter-sections: S2-S1 conical intersection in pyrazine. *Chem. Phys.* **2010**, *377*, 21.
  - [15] Myatt, C.J.; King, B.E.; Turchette, Q.A.; Sackett, C.A.; Kielpinski, D.; Itano, W.M.; Monroe, C.; Wineland, D.J. Decoherence of quantum superpositions through coupling to engineered reservoirs. *Nature* **2000**, *403*, 269.
  - [16] Piilo, J.; Maniscalco, S. Driven harmonic oscillator as a quantum simulator for open systems. *Phys. Rev. A* **2006**, *74*, 032303.

- [17] Tamascelli, D.; Smirne, A.; Huelga, S.F.; Plenio, M.B. Nonperturbative Treatment of non-Markovian Dynamics of Open Quantum Systems. *Phys. Rev. Lett.* **2018**, *120*, 030402.
- [18] Lemmer, A.; Cormick, C.; Tamascelli, D.; Schaetz, T.; Huelga, S.F.; Plenio, M.B. A trapped-ion simulator for spin-boson models with structured environments. *New J. Phys.* **2018**, *20*, 073002.
- [19] Demkowicz-Dobrzanski, R.; Jarzyna, M.; Kolodynski, J. Quantum Limits in Optical Interferometry. *Progr. Opt.* **2015**, *60*, 345.
- [20] Cavina, V.; Mancino, L.; Pasquale, A.D.; Gianani, I.; Sbroscia, M.; Booth, R.I.; Roccia, E.; Raimondi, R.; Giovannetti, V.; Barbieri, M. Bridging thermodynamics and metrology in nonequilibrium quantum thermometry. *Phys. Rev. A* **2018**, *98*, 050101(R).
- [21] Garbe, L.; Felicetti, S.; Milman, P.; Coudreau, T.; Keller, A. Metrological advantage at finite temperature for Gaussian phase estimation. *Phys. Rev. A* **2019**, *99*, 0.43815.
- [22] Razavian, S.; Paris, M.G.A. Quantum metrology out of equilibrium. *Phys. A* **2019**, *525*, 825.
- [23] Paris, M.G.A. Quantum estimation for quantum technology. *Int. J. Quant. Inf.* **2009**, *7*, 125.
- [24] Benedetti, C.; Paris, M.G.A. Characterization of classical Gaussian processes using quantum probes. *Phys. Lett. A* **2014**, *378*, 2495.
- [25] Zwick, A.; Alvarez, G.A.; Kurizki, G. Maximizing information on the environment by dynamically controlled qubit probes. *Phys. Rev. Appl.* **2016**, *5*, 014007.
- [26] Monras, A.; Paris, M.G.A. Optimal quantum estimation of loss in bosonic channels. *Phys. Rev. Lett.* **2007**, *98*, 160401.
- [27] Fujiwara, A. Quantum channel identification problem. *Phys. Rev. A* **2001**, *63*, 042304.
- [28] Fujiwara, A.; Imai, H. Quantum parameter estimation of a generalized Pauli channel. *J. Phys. A* **2003**, *36*, 8093.
- [29] Pinel, O.; Jian, P.; Treps, N.; Fabre, C.; Braun, D. Quantum parameter estimation using general single-mode Gaussian states. *Phys. Rev. A* **2013**, *88*, 040102.
- [30] Brida, G.; Degiovanni, I.P.; Florio, A.; Genovese, M.; Giorda, P.; Meda, A.; Paris, M.G.A.; Shurupov, A.P. Experimental estimation of entanglement at the quantum limit. *Phys. Rev. Lett.* **2010**, *104*, 100501.
- [31] Brida, G.; Degiovanni, I.P.; Florio, A.; Genovese, M.; Giorda, P.; Meda, A.; Paris, M.G.A.; Shurupov, A.P. Optimal estimation of entanglement in optical qubit systems. *Phys. Rev. A* **2011**, *83*, 052301.
- [32] Blandino, R.; Genoni, M.G.; Etesse, J.; Barbieri, M.; Paris, M.G.A.; Grangier, P.; Tualle-Brouiri, R. Homodyne estimation of Gaussian quantum discord. *Phys. Rev. Lett.* **2012**, *109*, 180402.
- [33] Benedetti, C.; Shurupov, A.P.; Paris, M.G.A.; Brida, G.; Genovese, M. Experimental estimation of quantum discord for a polarization qubit and the use of fidelity to assess quantum correlations. *Phys. Rev. A* **2013**, *87*, 052136.
- [34] Genoni, M.G.; Olivares, S.; Paris, M.G.A. Optical phase estimation in the presence of phase diffusion. *Phys. Rev. Lett.* **2011**, *106*, 153603.
- [35] Monras, A. Optimal phase measurements with pure Gaussian states. *Phys. Rev. A* **2006**, *73*, 033821.
- [36] Bina, M.; Allevi, A.; Bondani, M.; Olivares, S. Phase-reference monitoring in coherent-state discrimination assisted by a photon-number resolving detector. *Sci. Rep.* **2016**, *6*, 26025.

- [37] Kacprowicz, M.; Demkowicz-Dobrzański, R.; Wasilewski, W.; Banaszek, K.; Walmsley, I.A. Experimental quantum-enhanced estimation of a lossy phase shift. *Nat. Photonics* **2010**, *4*, 357.
- [38] Spagnolo, N.; Vitelli, C.; Lucivero, V.G.; Giovannetti, V.; Maccone, L.; Sciarrino, F. Phase estimation via quantum interferometry for noisy detectors. *Phys. Rev. Lett.* **2012**, *108*, 233602.
- [39] Brunelli, M.; Olivares, S.; Paris, M.G.A. Qubit thermometry for micromechanical resonators. *Phys. Rev. A* **2011**, *84*, 032105.
- [40] Correa, L.A.; Mehboudi, M.; Adesso, G.; Sanpera, A. Individual quantum probes for optimal thermometry. *Phys. Rev. Lett.* **2015**, *114*, 220405.
- [41] Stenberg, M.P.V.; Sanders, Y.R.; Wilhelm, F.K. Efficient estimation of resonant coupling between quantum systems. *Phys. Rev. Lett.* **2014**, *113*, 210404.
- [42] Bina, M.; Amelio, I.; Paris, M.G.A. Dicke coupling by feasible local measurements at the superradiant quantum phase transition. *Phys. Rev. E* **2016**, *93*, 052118.
- [43] Rossi, M.A.C.; Bina, M.; Paris, M.G.A.; Genoni, M.G.; Adesso, G.; Tufarelli, T. Probing the diamagnetic term in light-matter interaction. *Quantum Sci. Technol.* **2017**, *2*, 01LT01
- [44] Tamascelli, D.; Benedetti, C.; Olivares, S.; Paris, M.G.A. Characterization of qubit chains by Feynman probes. *Phys. Rev. A* **2016**, *94*, 042129.
- [45] Leggett, A.J.; Chakravarty, S.; Dorsey, A.T.; Fisher, M.P.A.; Garg, A.; Zwerger, W. Dynamics of the dissipative two-state system. *Rev. Mod. Phys.* **1987**, *59*, 1.
- [46] Shnirman, A.; Makhlin, Y.; Schön, G. Noise and decoherence in quantum two-level systems. *Phys. Scr.* **2002**, *T102*, 147.
- [47] Barndorff-Nielsen, O.E.; Gill, R.D. Fisher information in quantum statistics. *J. Phys. A* **2000**, *33*, 4481.